JOURNAL OF MAGNETIC RESONANCE 74, 177–183 (1987)

Simulation of the Cross-Peak Fine Structure in 2D NMR Spectroscopy by Analytical Calculation of the Density Operator in a Product Operator Basis

IMKE BOCK AND PAUL RÖSCH

Max-Planck-Institut für Medizinische Forschung, Abteilung Biophysik, Jahnstrasse 29, D-6900 Heidelberg, West Germany

Received March 25, 1987

In the last decade a great variety of pulse sequences has been developed using scalar or dipolar correlations between the spins of a molecule (*1*). The analysis of any pulse sequence can be simplified essentially by an analytical calculation of the density operator, the latter providing a survey over all appearing coherences at any predetermined time. For this purpose the program MARS was developed.

The program MARS provides the analytical calculation of the density operator after an arbitrary multiple-pulse excitation sequence, $\rho(t_f)$, and the simulation of 2D spectra of even the most complex amino acids. It is possible, for example, to calculate the cross peaks of leucine in D_2O, a spin system consisting of 10 spins, or of glutamic acid in D_2O, which exhibits eight coupling constants. The available computer memory may pose practical limitations for systems with more than eight spins and more than eight coupling constants.

The calculation is based on the product operator formalism described by Sørensen *et al.* (*2*) and van de Ven *et al.* (*3*) (in contrast to the calculations in, e.g., (*4*), which are based on numerical matrix calculations). The case of weak scalar coupling between several spin-$\frac{1}{2}$ particles is considered.

The calculation starts with the density matrix at thermal equilibrium, which is in the high temperature limit given by $\rho_0 = \Sigma_j I_z^j$. The time dependence of the density operator in the case that $\mathscr{H}$ is time-independent is given by the solution of the Liouville–von Neumann equation. The solution is

$$\rho(t_f) = e^{-i\mathscr{H}(t_f - t_i)/\hbar}\rho(t_i)e^{i\mathscr{H}(t_f - t_i)/\hbar}.$$

Here, $\rho(t_i)$ and $\rho(t_f)$ represent the initial and the final density operators. The density operator as well as $\mathscr{H}$ may be expressed as a linear combination of product operators. These are obtained by taking direct products of the single spin operators. The expectation value of the y component of the magnetization $\langle M_y \rangle = \gamma\hbar\langle I_y \rangle$ is given by

$$\langle M_y \rangle = \gamma\hbar \operatorname{Tr}\{\rho(t_f)I_y\}.$$

In a typical multiple-pulse experiment the Hamiltonian consists of a time-independent part ($\mathscr{H}_{CS} + \mathscr{H}_{SC}$) from chemical shifts and scalar couplings of the spins and a time-dependent part from interactions of the spins with RF fields when pulses are

0022-2364/87 $3.00

applied. Using the transformation to a frame rotating along the laboratory z axis (interaction representation) the high-frequency time dependence of $\mathscr{H}$ can be removed, $\mathscr{H} \rightarrow \mathscr{H}_{\text{eff}}$, and $\mathscr{H}$ becomes piecewise time-independent.

During the application of a strong RF pulse we may neglect $(\mathscr{H}_{\text{CS}} + \mathscr{H}_{\text{SC}})$. Thus $\mathscr{H}_{\text{eff}}$ reduces to $\mathscr{H}_{\text{eff}}^{\text{pulse}} = -\hbar\omega_1(I_x^j\cos\varphi + I_y^j\sin\varphi)$ which leads to the first transformation rule:

$$\rho(t_f) = e^{i\theta(I_x^j\cos\varphi + I_y^j\sin\varphi)}\rho(t_i)e^{-i\theta(I_x^j\cos\varphi + I_y^j\sin\varphi)}, \qquad [1]$$

where $\theta = \omega_1 t_p$; $\varphi = 0°$ represents an x pulse, $\varphi = 90°$, a y pulse.

The time evolution of the density operator during delays is determined by $(\mathscr{H}_{\text{CS}} + \mathscr{H}_{\text{SC}})$, leading to

$$\mathscr{H}_{\text{eff}}^{\text{delay}} = -\hbar\left(\sum_j \omega_j I_z^j + \sum_{j<k}\sum 2\pi J_{jk} I_z^j I_z^k\right).$$

Here, $\omega_j = \omega_{0j} - \omega_{\text{RF}}$ is the difference between the Larmor frequency and the RF frequency. Since terms due to chemical shift and scalar coupling in the Hamiltonian commute, the propagator $U = e^{-i\mathscr{H}_{\text{eff}}t/\hbar}$ can be factorized, which leads to the additional transformation rules:

$$\rho(t_f) = e^{\sum\sum_{j<k} i2\pi J_{jk} I_z^j I_z^k \tau}\rho(t_i)e^{-\sum\sum_{j<k} i2\pi J_{jk} I_z^j I_z^k \tau} \qquad [2]$$

for spin–spin coupling,

$$\rho(t_f) = e^{\sum_j i\omega_j I_z^j \tau}\rho(t_i)e^{-\sum_j i\omega_j I_z^j \tau} \qquad [3]$$

for chemical-shift effects.

The transformations $e^{i\lambda I_\alpha^j} I_\beta^j e^{-i\lambda I_\alpha^j}$ are well known, see, e.g., Slichter (*5*):

$$e^{i\lambda I_x} I_z e^{-i\lambda I_x} = I_z\cos\lambda + I_y\sin\lambda.$$

For every time interval where $\mathscr{H}_{\text{eff}}$ is constant, the successive application of these three transformations according to the pulse sequence yields the final density operator $\rho(t_f)$. It can be described by

$$\rho(t_f) = U_n \cdots U_2 U_1 \rho(t_i) U_1^{-1} U_2^{-1} \cdots U_n^{-1}.$$

The cross-peak fine structures of COSY 2D spectra show characteristic deletions when the flip angle of the mixing pulse is chosen smaller than 90° (*6*, *7*). The simulation of these characteristic deletions using the program MARS allows the recognition of the corresponding spin system in the spectrum of the molecule.

The major steps of the Pascal program MARS will now be described (Fig. 1). The number of spins k, the number of coupling constants, and the designations of the coupling constants are used as input parameters. Then a decision is made whether only a calculation of the density operator in terms of product operators is desired or whether the parameters for a graphical representation of the 2D spectrum should be calculated in addition. For a graphical output the numerical values of the coupling constants and the chemical shifts in hertz are required as input. Then the density operator at thermal equilibrium for the first designated spin is calculated. The next step is the specification of the arbitrary pulse sequence. Choosing an RF pulse, the pulse angle and the rotation axis (phase) have to be specified. Then the density operator $\rho(t_f)$ is calculated. After the second pulse a restriction of n-quantum transitions is possible.

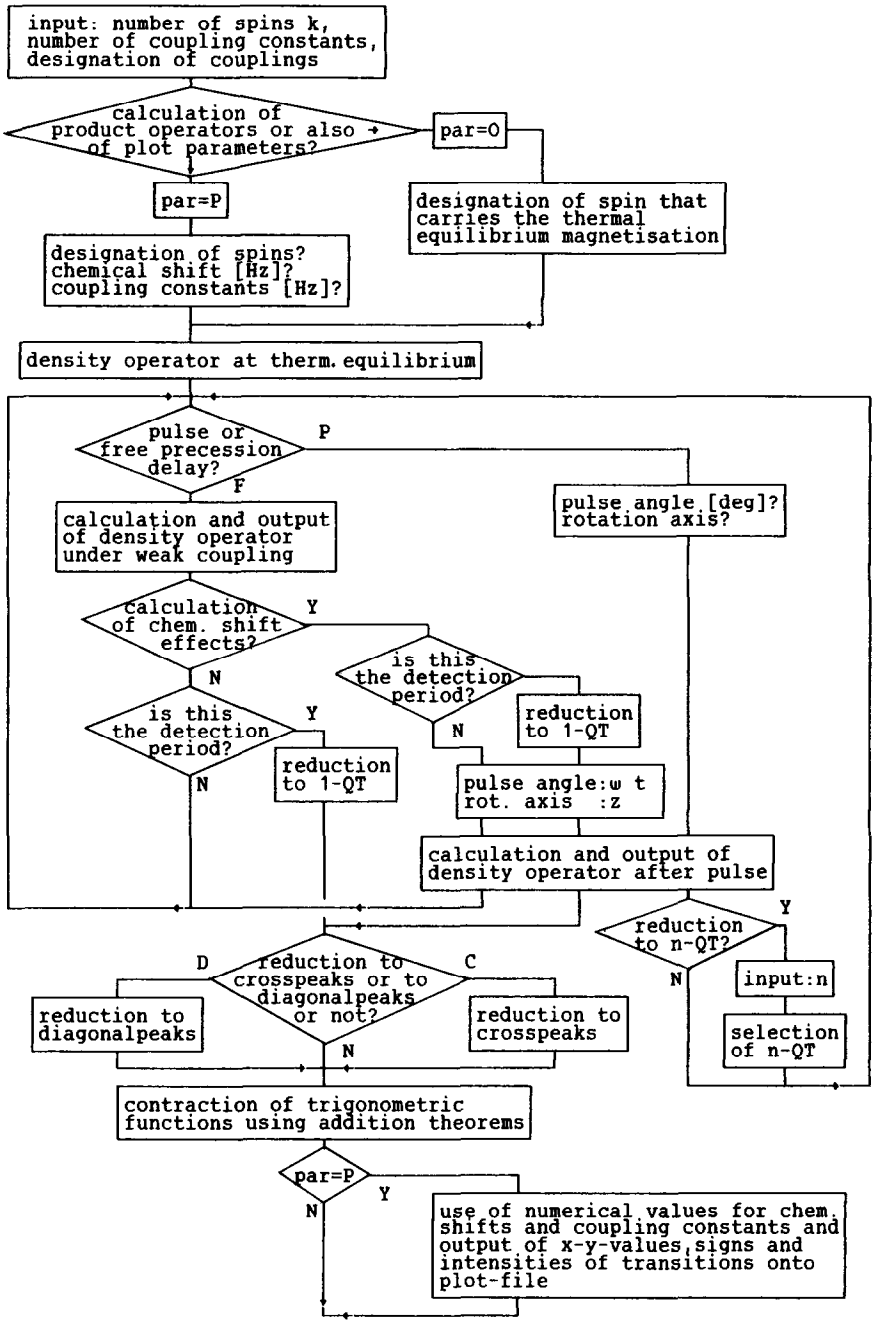

FIG. 1. Flow diagram of the program MARS.

For a free precession delay the density operator under the influence of all given scalar couplings will be calculated first. During every free precession period chemical-shift effects may be calculated or ignored; the latter feature is useful when refocusing 180° pulses are applied during this period. Chemical-shift effects are calculated as a pulse along the z axis with a pulse angle according to the nucleus whose chemical shift is considered, and according to the precession time of this period.

At this stage of the pulse sequence the number of terms representing the operators is proliferating, especially for multiple-quantum coherences. A simplification is possible for the detection period, where only the single-quantum transitions need to be considered. If the precession period calculated is the detection period a restriction to cross peaks or to diagonal peaks is included in the program as a possibility.

A typical output at this point of the program is represented, e.g., by the cross peaks of the A nucleus in Glu after the application of the COSY pulse sequence (Table 1 and Fig. 2):

RHO:=

−1My*sin WMt2*cos JMX2*cos JMT2*cos JMP2*sin JMA2
*sin WAt1*cos JAX1*cos JAT1*cos JAP1*sin JAM1
−1Py*sin WPt2*cos JPT2*cos JPM2*sin JPA2
*sin WAt1*cos JAX1*cos JAT1*sin JAP1*cos JAM1
−1Ty*sin WTt2*cos JTP2*cos JTM2*sin JTA2
*sin WAt1*cos JAX1*sin JAT1*cos JAP1*cos JAM1
−1Xy*sin WXt2*cos JXM2*sin JXA2
*sin WAt1*sin JAX1*cos JAT1*cos JAP1*cos JAM1

Here Py represents the y magnetization of the P nucleus P_y. Terms such as sin WPt2 denote sin $\omega_P t_2$, where t_i indicates the precession period, and cos JPT2

TABLE 1

Amino Acids, Corresponding Spin Systems, and the Couplings Measured in (*8*) Are Listed

Amino acid	Spin system	Scalar couplings
Gly	AX	J_{AX}
Ala	A_3X	J_{A_3X}
Thr	A_3MX	J_{A_3M}, J_{MX}
Val	A_3B_3MX	J_{A_3M}, J_{B_3M}, J_{MX}
Leu	A_3B_3MPTX	J_{A_3M}, J_{B_3M}, J_{PX}, J_{TX}
Ile	$A_3MPT(B_3)X$	J_{A_3M}, J_{A_3P}, J_{MT}, J_{PT}, J_{B_3T}, J_{TX}
{Ser}, Cys, Asp, Asn, Phe, Tyr, His, Trp	AMX	J_{AM}, $\{J_{AX}, J_{MX}\}$
Glu, {Gln}, [Met]	AM(PT)X	J_{AM}, $\{J_{AP}, J_{AT}, J_{MP}, J_{MT}, J_{PT}, [J_{AX}, J_{MX}]\}$
Pro, {Arg}	$A_2(T_2)MPX$	$J_{A_2T_2}$, J_{A_2M}, J_{A_2P}, $\{J_{PM}, J_{MX}, J_{PX}\}$
Lys	$A_2(F_2T_2)MPX$	$J_{F_2T_2}$, J_{MP}, J_{MX}, J_{PX}

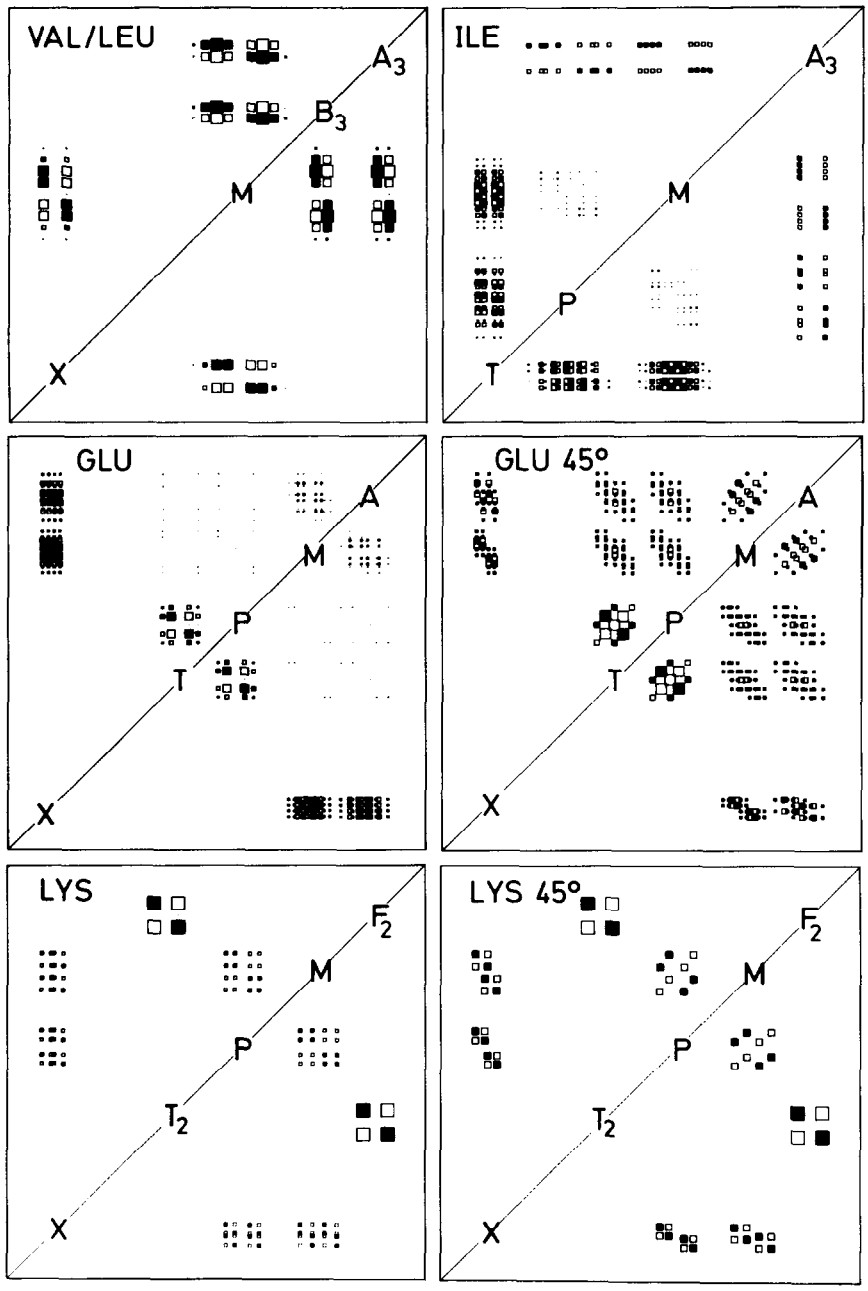

FIG. 2. Simulation of cross-peak patterns and fine structures for COSY and COSY-45° pulse sequences using the program MARS; ■, positive intensities; □, negative intensities.

symbolizes cos $\pi J_{PT} t_2$. Then the trigonometric functions will be contracted using addition theorems:

RHO:=

−,Py*cos(WPt2 − JPT2 − JPM2 − JPA2)
*cos(WAt1 − JAX1 − JAT1 − JAP1 − JAM1)
−,Py*cos(WPt2 − JPT2 − JPM2 − JPA2)
*cos(WAt1 − JAX1 − JAT1 − JAP1 + JAM1)
+,Py*cos(WPt2 − JPT2 − JPM2 − JPA2)
*cos(WAt1 − JAX1 − JAT1 + JAP1 − JAM1)
+,Py*cos(WPt2 − JPT2 − JPM2 − JPA2)
*cos(WAt1 − JAX1 − JAT1 + JAP1 + JAM1)
−,Py*cos(WPt2 − JPT2 − JPM2 − JPA2)
*cos(WAt1 − JAX1 + JAT1 − JAP1 − JAM1)
. . . (altogether 128 terms for the P nucleus).

This results again in a dramatic increase of the number of terms. The second character is a representative of the intensity of the transition "," → 1/128. In the last step the numerical values of coupling constants and chemical shifts are used to calculate the transition frequencies ω_1 and ω_2 as well as phases and intensities. These data are written to a plot file which is handled separately by a plot program.

For a graphical output the program is required to run k times to get all possible cross peaks. Each time the thermal equilibrium magnetization is assigned to only one spin but the same input parameters are used.

The program is running on a NORSK DATA computer ND500 and is currently adopted to the UNIX and MS.DOS operating systems. It is available on request.

Table 1, based on data measured in (*8*), is provided as a checklist for the input of the program. Amino acids, designation of the spin systems (*9*), and their couplings in D_2O (*8*) are listed. For the amino acids in brackets, only the couplings in brackets were measured. For all other amino acids all couplings written in the same line were resolved. Figure 2 shows COSY cross peaks of several amino acid spin systems. The mixing angles are either 45° or 90°.

The cross-peak fine structures of the amino acids Gly, Ala, Thr, and of AMX spin systems have been described (*10*, *11*). The square array of two positive and two negative peaks as in Gly is the fundamental pattern from which all multiplets are built up. The fine structure of the cross peaks corresponds to active coupling when the splitting is in antiphase in both frequency axes and to passive coupling when the splitting is in-phase along the appropriate axis. Figure 2 illustrates the branched amino acids valine or leucine where $J_{A3M} = J_{B3M} = \frac{1}{2}J_{MX}$ is chosen. They do not show mixing pulse effects. For a part of the isoleucine spin system A_3MPT using $J_{A3M} = J_{A3P} = \frac{1}{2}J_{PT} = \frac{3}{2}J_{MT}$ the mixing pulse effect is visible only if the geminal coupling J_{MP} is not equal to zero. Also, the complicated Glu spectrum is simulated using $J_{MX} = \frac{1}{2}J_{AX}$, J_{AM}

$= J_{PT} = -3J_{MX}$, $J_{AP} = J_{AT} = J_{MP} = J_{MT} = \frac{3}{2}J_{MX}$. The pattern of Lys where couplings to the A nucleus are left apart shows the influence of a COSY mixing pulse of less than 90° already known from AMX spin systems (*11*). On reduction of the mixing angle from 90° to 45° the directly connected transitions experience an increase in intensity in contrast to those that are not connected directly.

ACKNOWLEDGMENT

We thank Prof. Dr. U. Haeberlen for his encouragement and valuable discussions.

REFERENCES

1. R. R. ERNST, G. BODENHAUSEN, AND A. WOKAUN, "Principles of Nuclear Magnetic Resonance in One and Two Dimensions," Clarendon Press, Oxford, 1987.
2. O. W. SØRENSEN, G. W. EICH, M. H. LEVITT, G. BODENHAUSEN, AND R. R. ERNST, *Prog. NMR Spectrosc.* **16,** 163 (1983).
3. F. J. M. VAN DE VEN AND C. W. HILBERS, *J. Magn. Reson.* **54,** 512 (1983).
4. H. WIDMER AND K. WÜTHRICH, *J. Magn. Reson.* **70,** 270 (1986).
5. C. P. SLICHTER, "Principles of Magnetic Resonance," Springer-Verlag, Berlin, 1980.
6. G. BODENHAUSEN AND R. FREEMAN, *J. Magn. Reson.* **36,** 221 (1979).
7. S. SCHÄUBLIN, A. HÖHENER, AND R. R. ERNST, *J. Magn. Reson.* **13,** 196 (1974).
8. A. BUNDI AND K. WÜTHRICH, *Biopolymers* **18,** 285 (1979).
9. K. WÜTHRICH, "NMR of Proteins and Nucleic Acids," Wiley, New York, 1986.
10. D. NEUHAUS, G. WAGNER, M. VAŠÁK, J. H. R. KÄGI, AND K. WÜTHRICH, *Eur. J. Biochem.* **151,** 257 (1985).
11. A. BAX AND R. FREEMAN, *J. Magn. Reson.* **44,** 542 (1981).